Int J Adv Manuf Technol (2017) 93:3111–3123
DOI 10.1007/s00170-017-0775-2

ORIGINAL ARTICLE

Influence of laser heat treatment on microstructure and properties of surface layer of Waspaloy aimed for laser-assisted machining

Damian Przestacki[1] · **Mateusz Kukliński**[1] · **Aneta Bartkowska**[2]

Received: 8 April 2017 / Accepted: 30 June 2017 / Published online: 13 July 2017

Abstract In this study, a nickel-based superalloy, Waspaloy, was laser heat treated with diode laser. Single laser tracks were manufactured with different laser beam power densities between 63 and 331 kW/cm^2, and scanning laser beam speed ranged from 5 to 100 m/min. It was found that laser heat treatment of Waspaloy causes decrease in material hardness—the microhardness in laser tracks is about 300 HV0,1 while the microhardness of substrate is ranged from 300 to 600 HV0,1—which is a positive phenomenon for laser-assisted machining of investigated material. Impacts of laser heat treatment parameters on laser tracks properties were identified for obtaining multiple laser tracks with the most homogenous thickness. Moreover, roughness of heated layers was measured to specify surface quality after laser heat treatment. Multiple laser tracks were produced using different scanning laser beam speed and distances between laser tracks ranged from 0.125 to 1 mm. It was found that if scanning laser beam speed is 75 m/min and distance between laser tracks is equal to or lower than 0.25 mm, in microstructures of multiple laser tracks, cracks are occurring. The most suitable laser heat parameters for obtaining heated layers, and which can be used for laser-assisted machining, were identified as laser beam power density 178.3 kW/cm^2, scanning laser beam speed 5 m/min, and distance between laser tracks 0.125 mm.

✉ Damian Przestacki
damian.przestacki@put.poznan.pl

[1] Institute of Mechanical Technology, Poznan University of Technology, Piotrowo 3, 60-965 Poznan, Poland

[2] Institute of Material Science and Engineering, Poznan University of Technology, Jana Pawła II 24, 60-965 Poznan, Poland

Keywords Waspaloy · Diode laser · Laser heat treatment · Microstructure · Microhardness

1 Introduction

Since the discovery of methods to produce good quality nickel-based superalloys, they have been widely used in high-temperature and corrosive environments like those in aerospace engines and gas turbines. Due to increasing requirements for these units, manufacturers are constantly seeking for new solutions to boost properties of machine components and tools. These solutions include improvements in material compositions and manufacturing technologies [1–6]. Developments in nickel-based superalloy structure have led to production of Waspaloy. Its properties are a result of solid-solution strengthening elements (molybdenum, cobalt, and chromium) and age-hardening elements (aluminum and titanium) [7].

To improve components' properties, an ever increasing number of new technologies are applied. Because of its localized, fast heating, and controllability, laser treatment has gained in importance in metal industry and presently is applied in a variety of ways [8]. Laser cutting, welding, machining, etc. are widely used in automotive, aerospace, and electronic industries [9]. Lasers are also applied for heat treatment and alloying of metals' surfaces [10]. Moreover, laser heat treatment is one of the possibilities to improve the machining properties of materials which are hard to cut [11–15].

In manufacturing of nickel-based superalloys, lasers are used for welding and addictive manufacturing [16–19]. Furthermore, some of new research focuses on improving machinability of nickel-based alloys, including Waspaloy, by laser heat treatment. In fact, nickel-based alloys are particularly difficult to cut because of their superior mechanical properties and work-hardening phenomenon occurring. High stress developed

between the tool and workpiece during cutting generates deformed layer on metal surface [20].

Laser heat treatment carried out on nickel-based alloys for machining improvement is a reasonable solution considering changes of their properties in high temperatures. Waspaloy is good example of material which mechanical properties decrease if it is heated. Regardless of heat treatment applied on specific part, at 800 °C, tensile strength and 0.2% yield stress is about 50% lower than at room temperature [21].

Tadavani et al. show that machining Inconel 718 with laser assist dramatically reduces tool wear and specific cutting energy and improves surface roughness in comparison with conventional machining [22]. Similar research, carried out using Waspaloy by Ding and Shin [20], proves that tool wear and surface roughness are lower if machining is assisted with laser heat treatment.

There are significant microstructural changes in nickel-based alloys after laser heat treatment. Studies have found that laser shock processing of nickel-based alloys leads to nanocrystalline structure forming which solidification occurs epitaxially, perpendicular to the surface. Moreover, this structure offers good thermal stability, improved corrosion resistance, and fatigue strength increase [23, 24].

The objective of this article was to investigate the influence of laser heat treatment developed on surface of Waspaloy with various parameters and choose optimal parameters to manufacture layer for further machining. When choosing suitable parameters, the thickest and uniform layer thickness was demanded to remove as much as possible material in one operation. Furthermore, microstructure, microhardness, and roughness of layers were considered.

2 Research methodology

2.1 Material

Material used for the experiment was Waspaloy. Dimensions of examined specimens were 20 mm × 30 mm × 12 mm. Every specimen exhibited the roughness which was equal to S_a = 1.82 μm and S_z = 12.24 μm. Chemical composition of material is given in Table 1.

2.2 Laser heat treatment

For laser heat treatment of Waspaloy, diode laser TRUMPF TruDiode 3006 was used. This laser is based on single diode modules which allow to reach power of 3 kW. Laser was integrated with robot KUKA KR16-2, which allowed to control the location of laser beam accurately. The scheme of described system is presented in Fig. 1.

Table 1 Chemical composition of Waspaloy (wt%)

C	Cr	Co	Mo	Ti	Al	B	Fe	Ni
0.06	19.5	13.5	4.25	3.1	1.4	0.007	1	Bal.

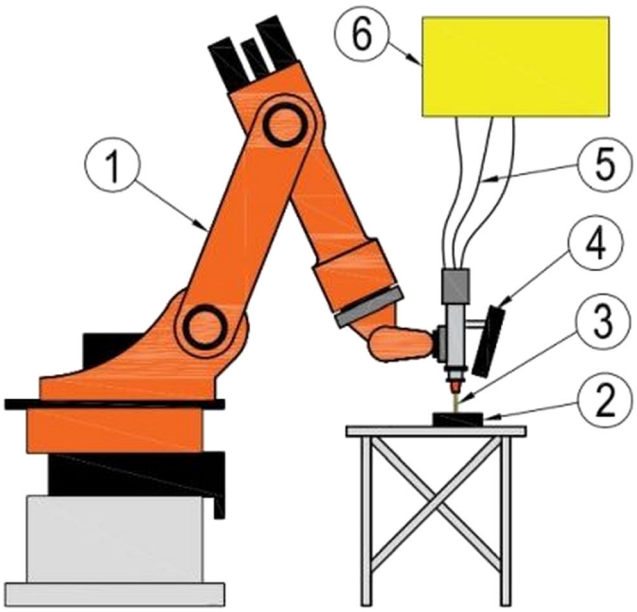

Fig. 1 Scheme of laser heat treatment process. *1* KUKA robot, *2* specimen, *3* laser beam, *4* pyrometer, *5* optic fibers, *6* optic resonator

Surface temperature during laser heat treatment was measured by RAYTEK MA1SC pyrometer which measuring range is 750–3000 °C and accuracy equal to ±3% of measured value. Measuring area was located 2 mm behind the laser beam, parallel to heating direction. The temperature measurement was carried out throughout the length of laser heat treatment which was 30 mm for each specimen. Before using the pyrometer, it

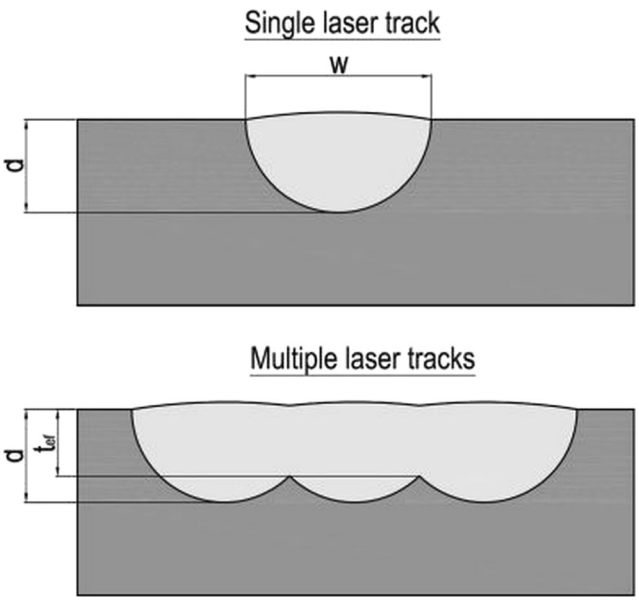

Fig. 2 Laser track dimension locations. *w* width of laser track, *d* depth of laser track, t_{ef} effective layer thickness

Table 2 Laser heat treatment parameters for manufacturing single laser tracks

P (W)	q (kW/cm^2)	v_l (m/min)
500	63.7	5
800	101.9	
1100	140.1	
1400	178.3	
1400	178.3	
1700	216.6	
2000	254.8	
2300	293.0	
2600	331.2	
1400	178.3	
1400	178.3	25
800	101.9	
1400	178.3	50
800	101.9	
1400	178.3	75
800	101.9	
1400	178.3	100
800	101.9	

was calibrated. For this purpose, steel samples heated throughout their volume were used. Their temperature was measured using the pyrometer and the thermometer integrated with the oven alternately, until these two values were equal.

2.3 Microstructure investigation

Microstructural research was carried out on laser tracks cross sections. Metallographic specimens were ground with abrasive papers of grit ranged from 120 to 2000 and subsequently polished using aluminum oxide suspension. For surface finishing, Marble's reagent was used. The light microscope (Carl Zeiss Metaval) equipped with camera (Moticam 2300 3.0 MP Live) and adequate software (Motic Images Plus 2.0 Resolution) was used to analyze the microstructural details.

During microstructure investigation, the dimensions of laser tracks were measured, using Axio Vision software. Measurements were taken on laser track cross sections. For single laser tracks, width and depth were measured; while for multiple laser tracks, the effective layer thickness was measured additionally. Locations of particular dimensions on laser tracks cross sections are shown in Fig. 2. Laser track width was measured on material surface and depth in track axes. The effective layer thickness was measured on boundaries of two adjacent laser tracks.

2.4 Microhardness and roughness testing

Microhardness testing was carried out with Zwick 3212B tester using load $F = 0.9807$ N. Roughness of surface after laser heat treatment was measured by profilographometer Hommel Tester H500. Additionally, images of 3D topography were made by profilographometer Hommel Tester H8000.

2.5 Experimental procedure

The research was split into four experimental series in which different input parameters were adjusted. The only one constant parameter was laser beam diameter (d_l) which was equal to 1 mm in each experiment. In the first two series, single laser tracks were produced with a different laser beam power P (ranged from 500 to 2600 W), for which laser beam power densities q (ranged from 63 to 331 kW/cm^2) have been calculated, and scanning laser beam speed v_l (ranged from 5 to

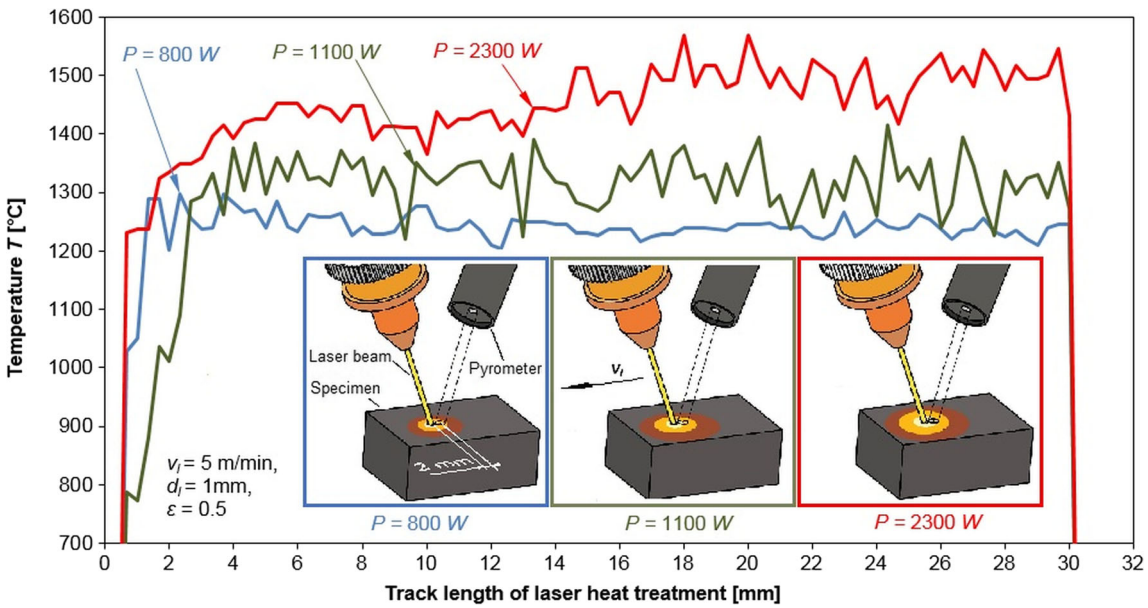

Fig. 3 Change in surface temperature depending on laser beam power

100 m/min), respectively. The details of laser heat treatment are shown in Table 2.

The analysis of single laser tracks has led to select laser heat treatment parameters for manufacturing multiple laser tracks in subsequent series. Multiple laser tracks were produced to determine the coverage of material surface by laser tracks and effective layer thickness homogeneity using different treatment parameters. Constant laser beam power and two different scanning laser beam speeds v_l = 5 m/min and v_l = 75 m/min were used. Adjusted parameters were number of laser tracks i (ranged from 4 to 32) and distance between them f (ranged from 0.125 to 1 mm). Moreover, an additional parameter—overlapping (O)—was introduced, on the basis of f values, to specify what percentage of laser track overlaps the previously manufactured one.

3 Results and discussion

3.1 Temperature measurement

Results of temperature measurements carried out during laser heat treatment of Waspaloy are shown in Fig. 3. Measurements were done for three different laser beam powers P = 800 W, P = 1100 W, and P = 2300 W, which correspond to laser beam power densities q = 101.9 kW/cm^2, q = 140.1 kW/cm^2, and q = 293 kW/cm^2. Scanning laser beam speed v_l = 5 m/min was constant, also laser beam diameter d = 1 mm, and emissivity ε = 0.5. The lowest value of temperature was measured with laser beam power equal to 800 W and the highest with 2300 W. With laser beam power of 800 W, the temperature oscillated between 1200 and 1300 °C. Laser beam power increase to 1100 W caused increase of temperature to the range from 1200 to 1300 °C. During research carried out with laser beam power P = 2300 W, pyrometer indicated values from 1350 to 1600 °C. Additionally, the location of pyrometer during the measurement, which was 2 mm behind the laser beam, and heat affected areas are schematically shown in Fig. 3.

3.2 Single laser tracks microstructure

Heat treatment changes the microstructure of alloy, and the properties are determined by the microstructure. The purpose of this paper was to investigate structure changes caused by laser heat treatment which can increase the machinability of Waspaloy. Some works [20], as well as our own experience

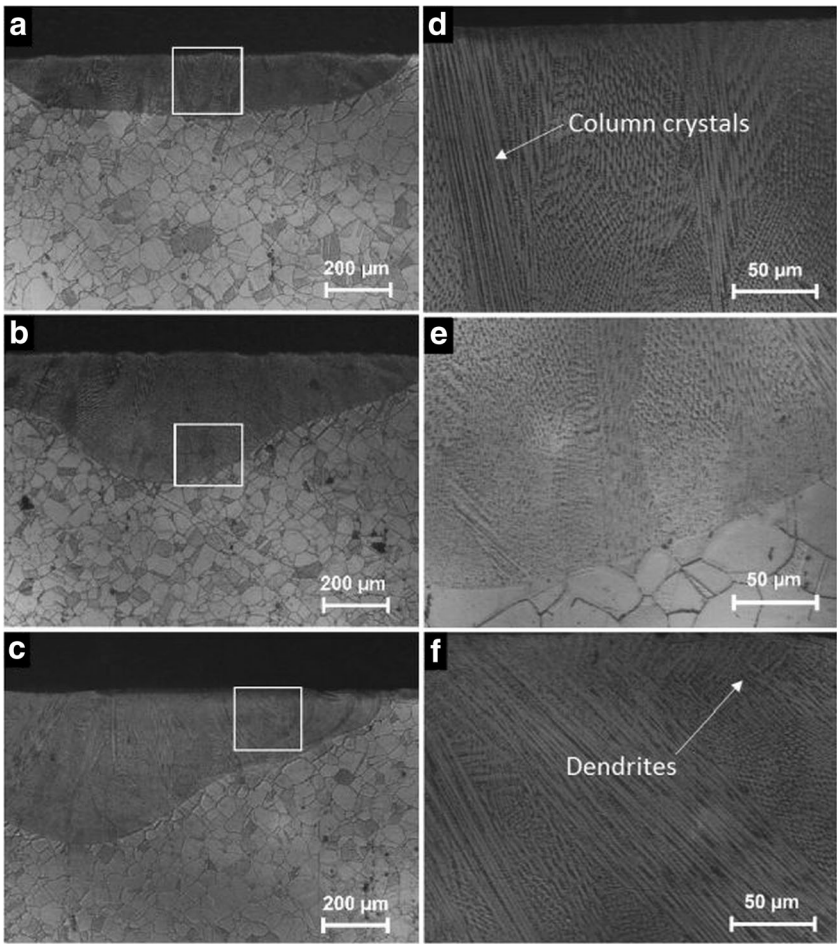

Fig. 4 Microstructures of single laser tracks manufactured with v_l = 5 m/min and different laser beam power densities q. **a** and **d** 101.9 kW/cm^2. **b** and **e** 178.3 kW/cm^2. **c** and **f** 331.2 kW/cm^2

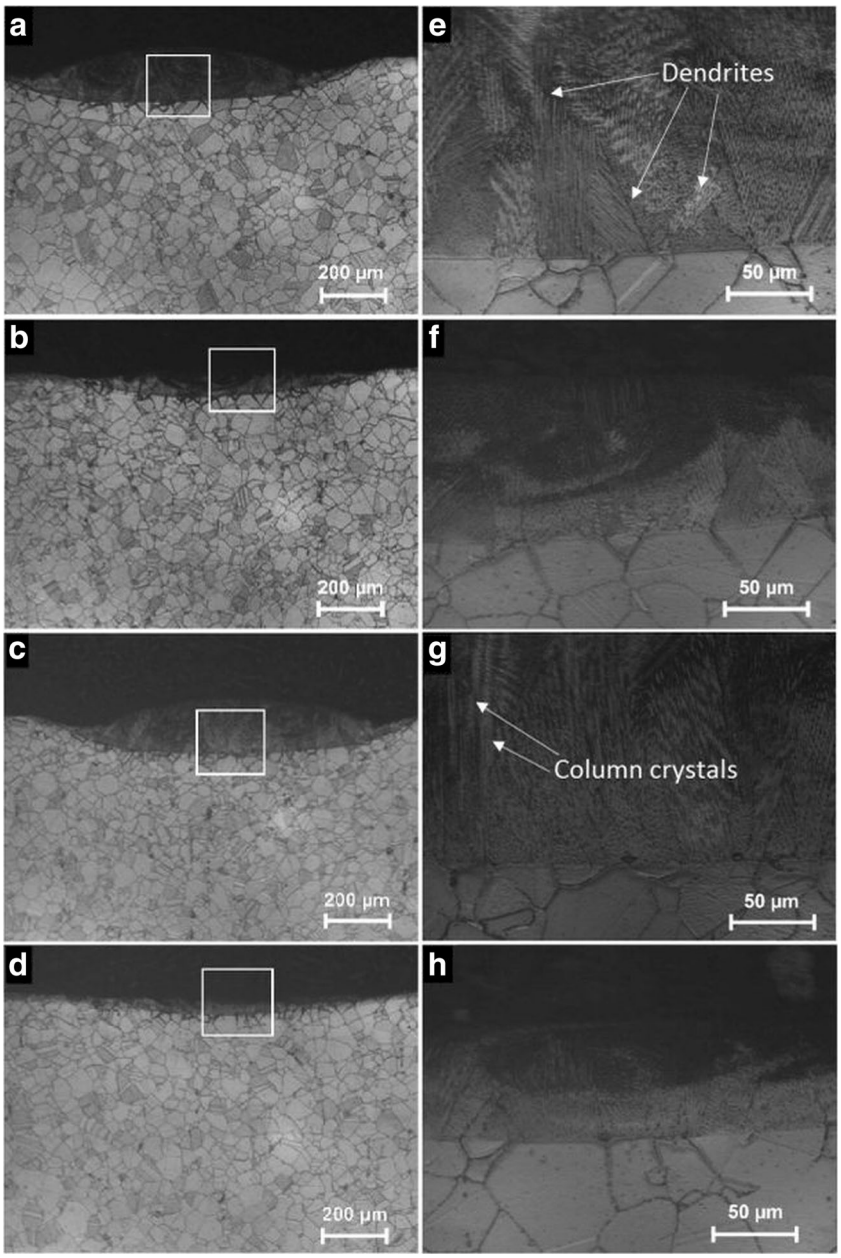

Fig. 5 Microstructures of single laser tracks manufactured with **a** and **e** q = 178.3 kW/cm^2 and v_l = 75 m/min; **d** and **f** q = 101.9 kW/cm^2 and v_l = 75 m/min; **c** and **g** q = 178.3 kW/cm^2 and v_l = 100 m/min; and **d** and **h** q = 101.9 kW/cm^2 and v_l = 100 m/min

[2, 11], show that laser modification of metals which are hard-to-cut leads to their better machinability.

After carrying out the analysis of microstructure and dimensions' measurements on all manufactured laser tracks, some images of them were chosen for representation. These are shown in Figs. 4a–f and 5a–h and were produced with laser beam power density ranged from 101.9 to 331.2 kW/cm^2 and scanning laser beam speed ranged from 5 to 100 m/min.

Microstructures of selected laser tracks manufactured with constant scanning laser beam speed and various laser beam power densities are shown in Fig. 4a–f. Microstructures shown in Fig. 4d–f are magnified areas marked in Fig. 4a–c. It was concluded that increasing laser beam power density results in increasing the size of laser tracks. Moreover, there are strict boundaries between heated zones and the core of material. It shows that the heat of laser beam is highly concentrated and heat dissipation is so quick that heat affected zones do not occur. Last but not least, in Fig. 4a–f, it is clearly shown that laser tracks grow with increasing laser beam power density.

The morphology of areas where material was heated includes column crystals oriented in the direction of heat dissipation which was perpendicular to the heating direction. With sufficient high subcooling, the form of crystals is transforming, and characteristic for dendritic growth second-order branches is appearing. Moreover, as the laser beam power increases, column and dendritic crystals become longer. Typical column-dendritic structure is visible in Fig. 4d–f. We predict that the

size of obtained dendrites influences the microhardness, and the bigger are the dendrites, then probably the lower the microhardness of treated surface.

On the basis of phase diagrams including nickel, it was figured that the phase composition of laser tracks includes mainly nickel, α-cobalt with face-centered cubic structure, ε-cobalt with hexagonal close-packed structure, and mixtures of these and other alloying elements (Table 3).

Laser tracks presented in Fig. 5a–h were manufactured with different scanning laser beam speeds. Microstructures shown in Fig. 5e–h are magnified areas marked in Fig. 5a–d. Comparing Fig. 5a with c and b with d, it can be clearly seen that increasing scanning laser beam speed causes laser tracks width and depth decrease. Besides that, in comparison with laser tracks manufactured with constant scanning laser beam speed, laser tracks manufactured with constant laser beam power density are characterized by higher material shrinkage. Moreover, surfaces of laser tracks shown in Fig. 5a–h are lens-shape, while laser tracks manufactured with lower scanning laser beam speed (Fig. 4a–f) are smooth.

For laser tracks produced with higher scanning laser beam speed, equal to 100 m/min, areas with much different light reflectiveness occurred. The reason of this is formation of dendrites with various crystal orientations. These differences in orientation derive from higher range of concentration supercooling, which allowed to free dendritic growth. Moreover, during such quick solidification, phases existing in the volume of laser tracks get trapped in random areas emerged by melted material convection.

3.3 Single laser track dimensions

In Figs. 6 and 7, influences of laser heat treatment parameters on width and depth of laser tracks are shown. The use of higher laser beam power density causes more heat supply to material, which leads to melt its higher volume. In this research, depths of laser tracks were ranged from 200 to 750 μm. The deepest laser track was produced with $q = 254.8$ kW/cm^2 ($P = 2000$ W) and the widest one with $q = 293$ kW/cm^2 ($P = 2300$ W).

Table 3 Laser heat treatment parameters for manufacturing multiple laser tracks

P (W)	q (kW/cm^2)	v_l (m/min)	d_l (mm)	f (mm)	i	O (%)
1400	178.3	5	1	1.00	4	0
				0.50	8	50
				0.25	16	75
				0.125	32	87.5
		75	1	1.00	4	0
				0.50	8	50
				0.25	16	75
				0.125	32	87.5

After analysis of microstructures and dimensions of laser tracks manufactured with constant scanning laser beam speed, two laser beam power densities, equal to 101.9 and 178.3 kW/cm^2, were selected for further examination which determines influence of scanning laser beam speed on Waspaloy properties.

It was concluded that using higher scanning laser beam speed leads to a decrease in laser track dimensions. This phenomenon can be seen comparing Figs. 4b and 5a and c in which laser tracks produced with three different scanning laser beam speed are shown, and Fig. 5b and d related to specimens manufactured with $q = 101.9$ kW/cm^2.

The slope of approximation line in Fig. 6 is higher than in Fig. 7. It means that laser beam power density has higher influence on size of laser tracks than scanning laser beam speed has.

3.4 Single laser track microhardness

Microhardness testing was carried to identify how microstructural changes, accomplished with laser heat treatment, impact on mechanical properties of Waspaloy. For each laser track, several indentations were made and measured. The number of indentations depended on laser track depth. The exemplary locations of indentations, made on cross sections of laser track manufactured with $v_l = 5$ m/min and $q = 178.3$ kW/cm^2, are shown in Fig. 8.

The next step was to count the average value of microhardness of laser tracks and base material. These values are shown in Figs. 9 and 10. Microhardness changes in specimens which were produced with constant scanning laser beam speed are shown in Fig. 9. Microhardness changes in specimens manufactured with different scanning laser beam speeds are shown in Fig. 10.

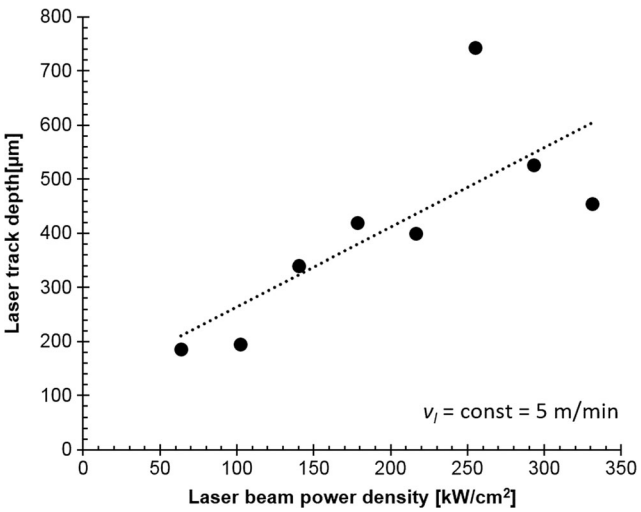

Fig. 6 The influence of laser beam power density (q) on the depth of single laser tracks manufactured with constant scanning laser beam velocity $v_l = 5$ m/min

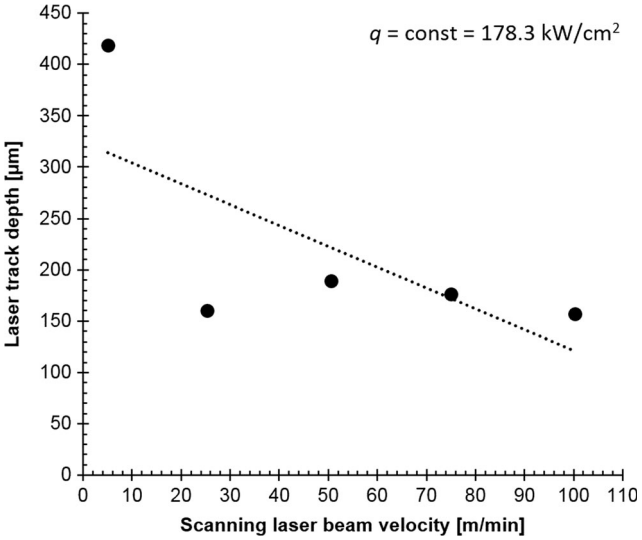

Fig. 7 The influence of scanning laser beam velocity (v_l) on the depth of single laser tracks manufactured with constant laser beam power density q = 178.3 kW/cm^2

In most cases, laser heat treatment leads to an increase in material hardness. For Waspaloy, obtained structure after laser modification has lower hardness than base material. The reason of this phenomenon is dendritic structure which is characterized by lower durability and worse mechanical properties, e.g., hardness, due to large grain size. Moreover, the size of obtained dendrites has influence on the microhardness. As can be seen in Fig. 4, sample manufactured using higher laser beam power density (Fig. 4c) has bigger dendrites and its microhardness is slightly lower (Fig. 9) than this which was manufactured with lower laser beam power density (Fig. 4a). Additionally, the carbides and nitrides present in structure are melted during laser heat treatment, and the chemical composition and microhardness become more homogenous.

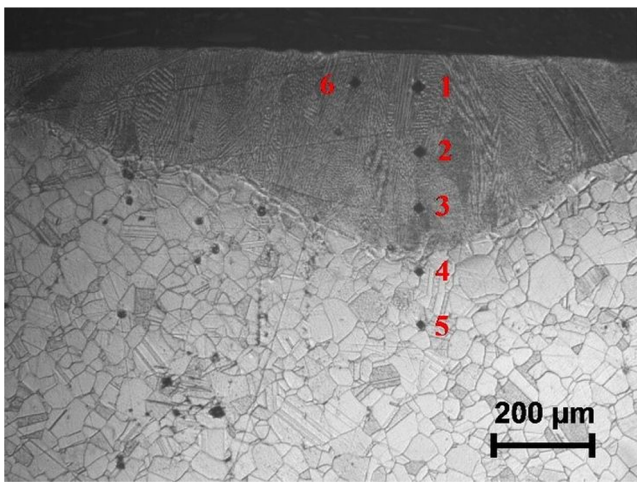

Fig. 8 Exemplary locations of indentations emerged during Vickers microhardness testing

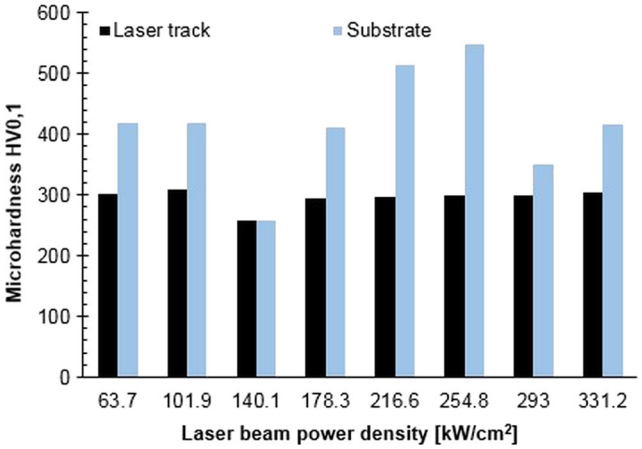

Fig. 9 The influence of laser heat treatment carried out with different laser beam power densities and constant scanning laser beam velocity v_l = 5 m/min on microhardness HV0,1

The effect of decreasing the microhardness by laser heat treatment is essential for reducing cutting energy and tool wear during further machining. Laser heat treatment with constant scanning laser beam speed caused about 25% decrease in microhardness regardless of the laser beam power density used. Moreover, microhardness of laser tracks is similar, equal to approximately 300 HV0,1. On the other hand, second experimental series revealed that microhardness of laser tracks depends on scanning laser beam speed (Fig. 10). The higher scanning laser beam speed, the higher microhardness of laser track.

Multiple laser tracks were produced to examine properties of heated layers using different distances between single laser tracks. As a result of analyzing dimensions and properties of single laser tracks, laser beam power density equal to 178.3 kW/cm^2 was selected to manufacture heated layers. Microstructures of multiple laser tracks produced with two different scanning laser beam speeds are shown in Figs. 11 and 12.

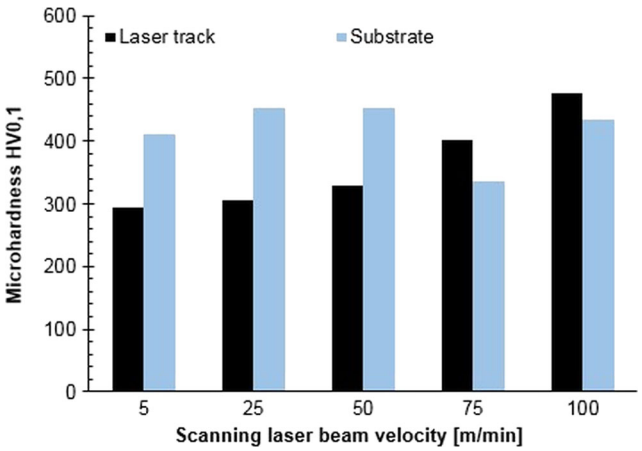

Fig. 10 The influence of laser heat treatment carried out with different scanning laser beam velocities and constant laser beam power density q = 178.3 kW/cm^2 on microhardness HV0,1

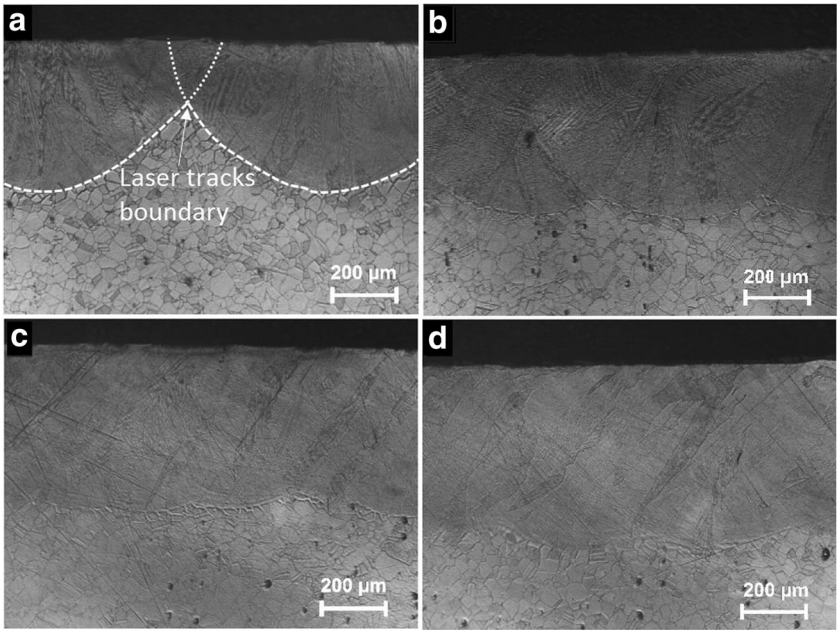

Fig. 11 Microstructures of multiple laser tracks manufactured with q = 178.3 kW/cm^2, v_l = 5 m/min, and different distances between laser tracks. **a** f = 1 mm. **b** f = 0.5 mm. **c** f = 0.25 mm. **d** f = 0.125 mm

3.5 Multiple laser track microstructure

Multiple laser tracks manufactured with scanning laser beam speed equal to 5 m/min are characterized by homogenous structures. In areas where particular laser tracks are overlapped, mixed grain orientation was found. These various orientations resulted from slightly different crystallization directions in each laser track.

In Fig. 12c and d, multiple cracks can be seen in produced heated layers. These cracks appeared between subsequent laser tracks. Some of these cracks are as long as heated layer thickness. This effect makes heated layers produced with scanning laser beam speed v_l = 75 m/min and distances between laser tracks equal to 0.25 and 0.125 mm unsuitable for further machining. Such long and densely appearing cracks create risk of spreading into base material during the machining process.

Multiple cracks appearing in heated layers manufactured with high scanning laser beam speed and short distances between laser tracks are result of high heat dissipation and stress occurring in material during quick solidification. If laser heat treatment is conducted with low-scanning laser beam speed v_l = 5 m/min, the heat affects unit surface for longer, which leads to slower solidification and stress disappearance.

Multiple laser tracks produced with scanning laser beam speed equal to 75 m/min are unsuitable for further machining

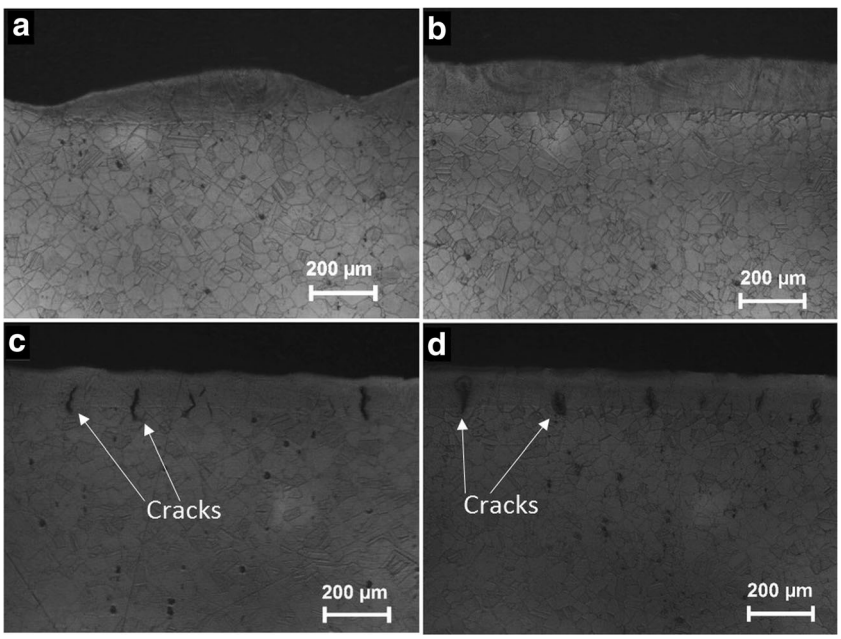

Fig. 12 Microstructures of multiple laser tracks manufactured with q = 178.3 kW/cm^2, v_l = 75 m/min, and different distances between laser tracks. **a** f = 1 mm. **b** f = 0.5 mm. **c** f = 0.25 mm. **d** f = 0.125 mm

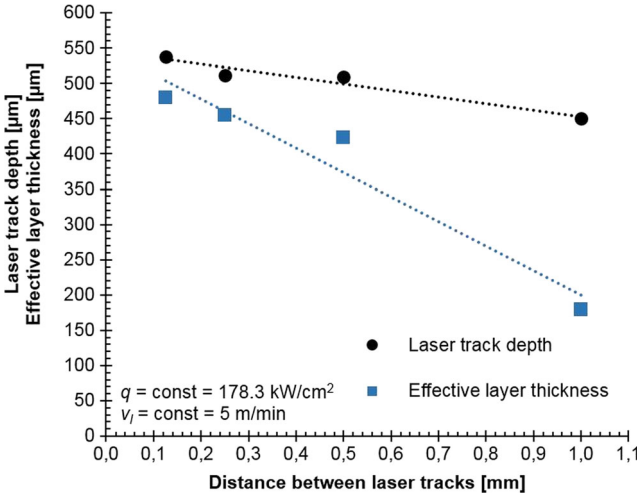

Fig. 13 The influence of distance between laser tracks on depth and effective thickness for heated layers manufactured with q = 178.3 kW/cm^2 and v_l = 5 m/min

regardless of distance between single laser tracks. If distances between single laser tracks are higher than 0.5 mm, effective layer thickness is too short for further machining. On the other hand, if single laser tracks are closer, multiple cracks are occurring, which could highly worsen properties of material surface after machining.

3.6 Multiple laser track dimensions

Multiple-affecting material with laser beam was aimed to manufacture homogenous and, as thick as possible, heated layers. This is particularly important because of further material machining. The higher effective layer thickness, the more material can be cut out in one operation.

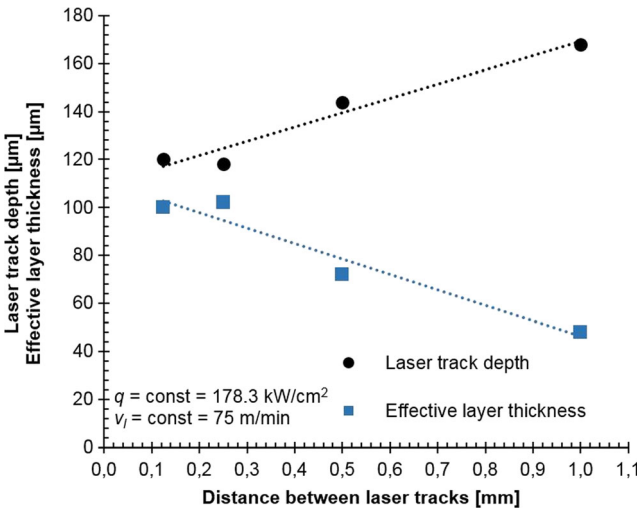

Fig. 14 The influence of distance between laser tracks on depth and effective thickness for heated layers manufactured with q = 178.3 kW/cm^2 and v_l = 75 m/min

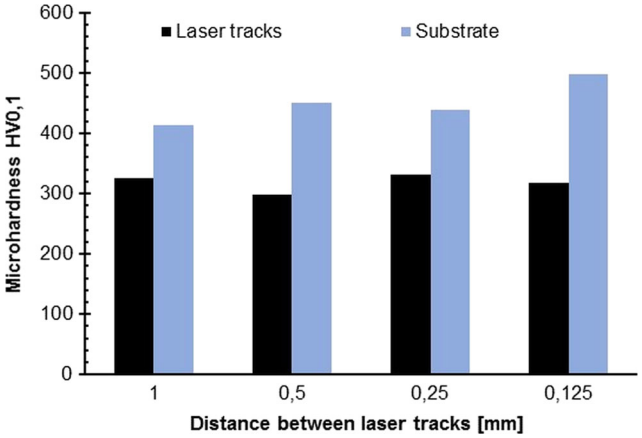

Fig. 15 Microhardness of substrate and multiple laser tracks manufactured with v_l = 5 m/min

It was essential to manufacture heated layers in which effective layer thicknesses are as close as possible to single laser track depths. Manufacturing of heated layers in which there is much difference between effective layer thickness and laser tracks depth is highly uneconomical because material removed while further machining is as deep as effective layer thickness. Furthermore, in this case, areas of higher hardness occur between laser tracks, which leads to severe tool wear.

In Figs. 13 and 14, an influence of distance between laser tracks on depth and effective thickness of heated layers is shown. Considering described requirements for laser track depth and effective layer thickness, the most suitable dimensions were obtained on specimen which distance between laser tracks was equal to 0.125 mm and scanning laser beam speed was 5 m/min. In this case, the highest laser track depth and effective layer thickness were obtained. Moreover, effective layer thickness is about 90% of laser track depth, which means that almost entire heated area can be removed in one operation.

With the increasing distance between laser tracks, dimensions of single laser tracks decrease. This concerns both laser

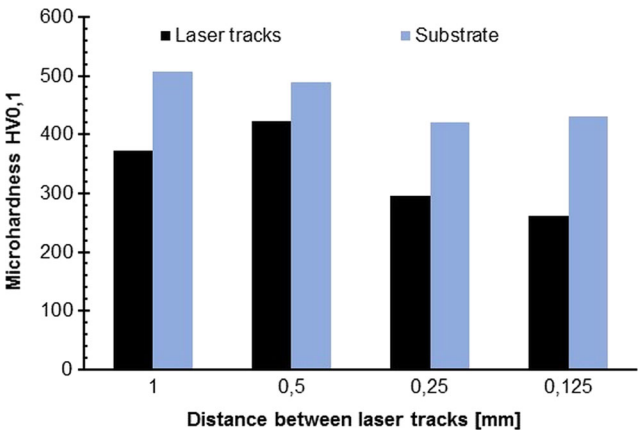

Fig. 16 Microhardness of substrate and multiple laser tracks manufactured with v_l = 75 m/min

Table 4 Heated layer surface roughness

q (kW/cm^2)	v_l (m/min)	f (mm)	S_a (μm)	S_z (μm)
178.3	5	1.00	2.8	27.6
		0.50	2.1	19.8
		0.25	2.2	24.2
		0.125	2.0	21.6
	75	1.00	10.0	86.6
		0.50	4.6	41.8
		0.25	5.6	50.1
		0.125	1.9	20.2

track depth and effective layer thickness which is shown in Fig. 13. The actual vision of this relation is shown in Fig. 11.

Increasing scanning laser beam speed from v_l = 5 m/min to v_l = 75 m/min causes manufactured laser track dimensions shrinkage. Because the width of single laser track produced with v_l = 75 m/min is lower, adjacent laser tracks do not overlap and affect each other. Due to this phenomenon, if higher scanning laser beam speed is used, laser track depth increases and effective layer thickness decreases with the increase of distance between laser tracks.

3.7 Multiple laser track microhardness

Microhardness of Waspaloy has decreased using both scanning laser beam speed v_l = 5 m/min and v_l = 75 m/min. The results are shown in Figs. 15 and 16. In Fig. 15, microhardness of substrate and multiple laser tracks manufactured with v_l = 5 m/min is shown and in Fig. 16—with v_l = 75 m/min.

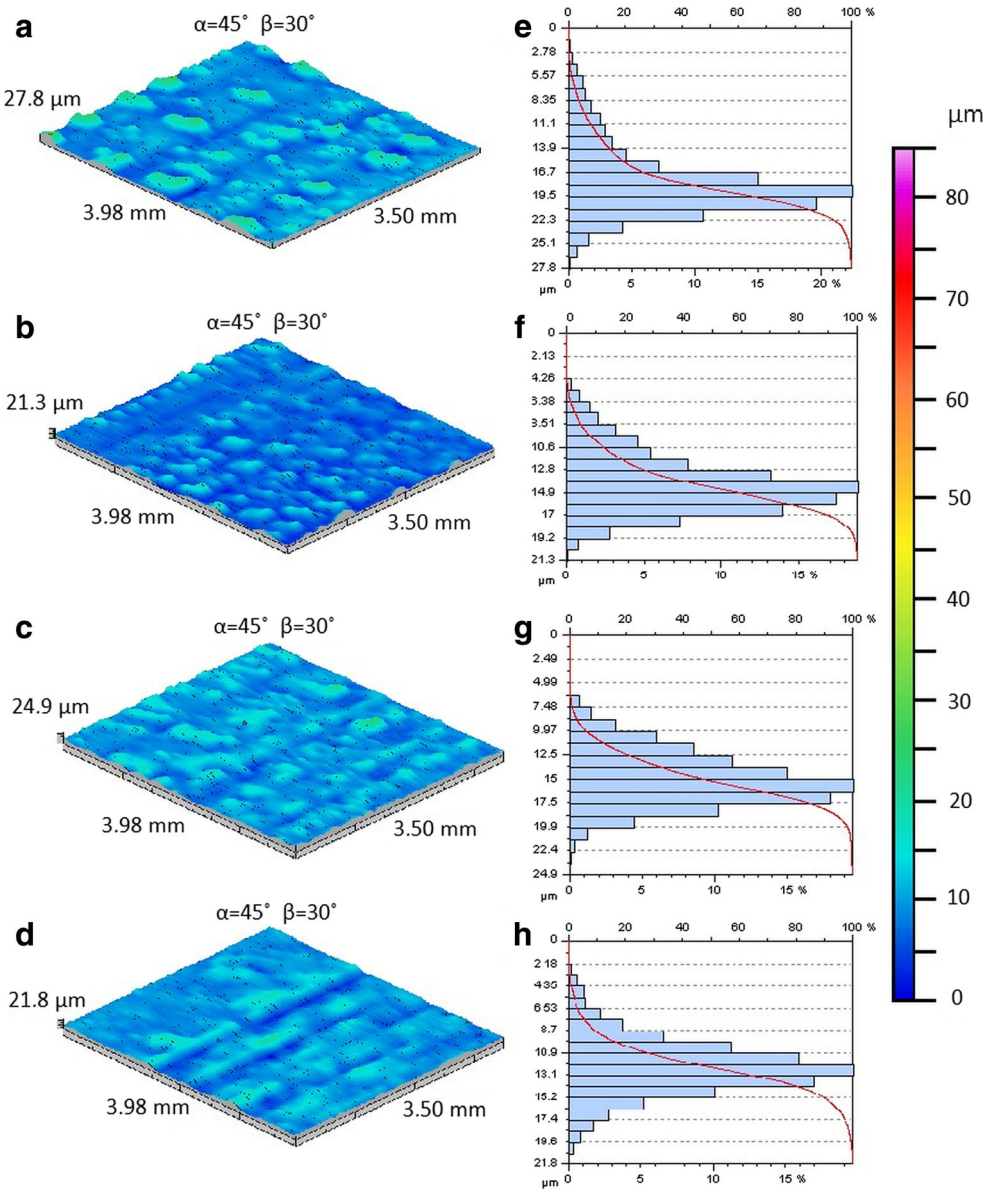

Fig. 17 Roughness profiles and surface peak distributions of multiple laser tracks manufactured with q = 178.3 kW/cm^2, v_l = 5 m/min. **a** and **e** f = 1 mm. **b** and **f** f = 0.5 mm. **c** and **g** f = 0.25 mm. **d** and **h** f = 0.125 mm

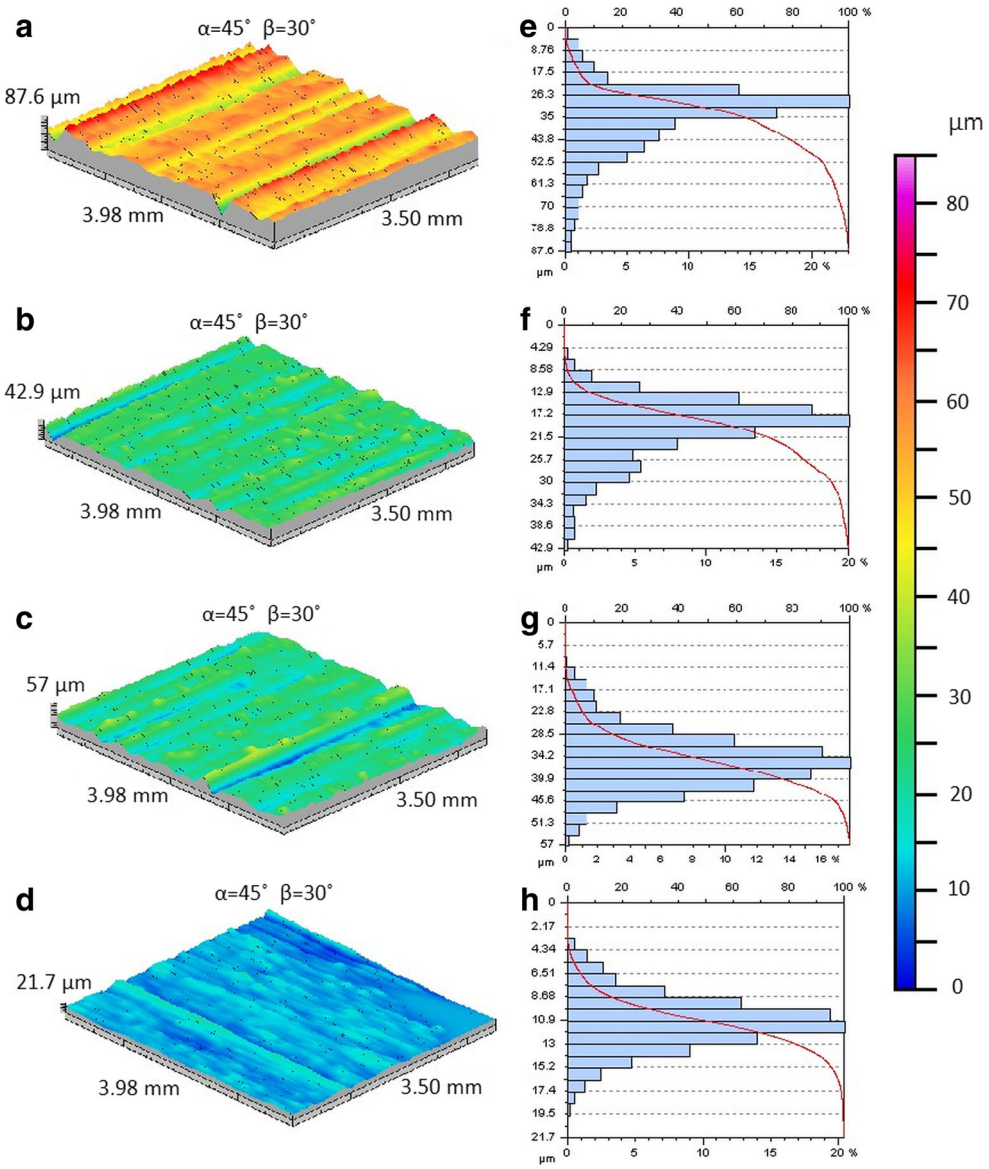

Fig. 18 Roughness profiles and surface peak distributions of multiple laser tracks manufactured with $q = 178.3$ kW/cm^2, $v_l = 75$ m/min. **a** and **e** $f = 1$ mm. **b** and **f** $f = 0.5$ mm. **c** and **g** $f = 0.25$ mm. **d** and **h** $f = 0.125$ mm

As in case of single laser tracks, manufacturing of multiple laser tracks also led to obtaining a dendritic microstructure with lower microhardness. The most decrease in Waspaloy microhardness was found in specimens with laser tracks manufactured with distance between them $f = 0.125$ mm. In this case, when $v_l = 5$ m/min was used, laser heat treatment caused 36% hardness decrease, and with $v_l = 75$ m/min, hardness has lowered by 40%. It was found that the level of hardness decrease is independent from distance between laser tracks.

3.8 Surface roughness on multiple laser tracks

To determine surface quality after manufacturing heated layers of Waspaloy, surface roughness on multiple laser tracks was measured. The obtained results—roughness parameters S_a and S_z—are shown in Table 4. S_a parameter is an average roughness deviation, and S_z is a ten-point surface irregularity height. Moreover, 3D representations of selected heated layer surfaces and surface irregularity distributions are shown in Figs. 17 and 18. Values given in micrometers near roughness profiles are maximal peak heights measured on an adequate specimen.

Surface is more smooth on heated layers manufactured with lower scanning laser beam speed. Their measured roughness parameters S_z are ranged from approximately 20 to 28 µm. Maximal peak height is 27.8 µm. S_z parameters of laser tracks manufactured with $v_l = 75$ m/min are ranged from approximately 20 to 90 µm. It was found that the surface roughness decreases if laser tracks are closer to each other—regardless of scanning laser beam speed. The smoothest surface was obtained by manufacturing laser tracks with scanning laser beam speed 5 m/min and distance between them equal to 0.5 mm.

Analyzing peak height distributions in specimens manufactured with $v_l = 5$ m/min (Fig. 17e–h) led to spot that the most numerous peak heights constitute from 60 to 70%

of maximal height values. Using 15 times higher scanning laser beam speed (v_l = 75 m/min) caused a decrease of ratio between the most numerous and the highest peaks. As it is shown in Fig. 18e–h, the percentage of the most numerous peak heights is ranged from 30 to 60% of maximal peak heights. This phenomenon signals that roughness increase goes in parallel with greater surface heterogeneity.

4 Conclusions

This paper presents an investigation of laser heat treatment influence on Waspaloy aimed to laser-assisted machining. Results of this research led to following conclusions:

(1) Laser heat treatment of Waspaloy decreases its hardness, and this phenomenon allows using laser for machining assist of this material. Exception to this principle is laser heat treatment with scanning laser beam speed greater than or equal to 75 m/min which hardens the surface.
(2) It was found that hardness of laser heat-treated Waspaloy does not depend on laser beam power used; however, it depends on scanning laser beam speed and the higher the scanning laser beam speed, the harder the surface.
(3) The most suitable dimensions of layers treated with diode laser for further laser-assisted machining of Waspaloy were obtained by using following laser heat treatment parameters: q = 178.3 kW/cm^2, v_l = 5 m/min, and f = 0.125 mm. With these parameters used, the highest laser track depth and effective layer thickness were obtained. Moreover, effective layer thickness was about 90% of single laser track depth, which allows to remove almost entire laser-treated volume of material without the risk of increasing tool wear due to exposing it to areas with various hardness.
(4) Layers manufactured by multiple laser heat treatment carried out with scanning laser beam speed greater than or equal to 75 m/min, and distances between single laser tracks lower than 0.5 mm are unsuitable for assisting machining of Waspaloy. Laser heat treatment with mentioned parameters leads to multiple cracks appearing in the treated area which can be critical for material surface after machining.
(5) Boosting scanning laser beam speed of laser heat treatment causes increasing surface roughness. It was also found that surface roughness increases with distance between single laser track extension.

Acknowledgements The presented research results, executed under the domestic project PBS of No. 244445, were funded with grants for education allocated by the National Centre for Research and Development.

References

1. Dul I (2013) Application and processing of nickel alloys in the aviation industry. Weld Int 27:48–56
2. Przestacki D, Jankowiak M (2014) Surface roughness analysis after laser assisted machining of hard to cut materials. J Phys Conf Ser 483(012019):1–7
3. Yi-feng X., Wen-hu W., et. al. (2016), Surface integrity of milling in-situ TiB2 particle reinforced Al matrix composites. Int J of Refractoty Metels and Hard Mater 54: 407–416
4. Kunyang L., Wenhu W., et. al. (2017) Grindability and surface integrity of in situ TiB2 particle reinforced aluminum matrix composites. [J] Int J Adv Manuf Technol 88(1): 887–898
5. Tseng SF, Hsiao WT, Huang KC, Chen MF, Lee CT, Chou CP (2010) Characteristics of Ni-Ir and Pt-Ir hard coatings surface treated by pulsed Nd:YAG laser. Surf Coat Tech 205(7):1979–1984
6. Rahsepar M, Bahrololoom ME (2009) Study of surface roughness and corrosion performance of Ni/Zn-Fe and Zn-Fe/Ni compositionally modulated multilayer coatings. Surf Coat Tech 204(5):580–585
7. Razavi RS (2016) Laser beam welding of Waspaloy: characterization and corrosion behavior evaluation. Opt Laser Technol 82:113–120
8. Kotlan V, Hamar R, Pánek D (2016) Combined heat treatment of metal materials, COMPEL 35. Iss 4:1450–1459
9. Steen WM (2010) Laser Material Processing:172–219
10. Bartkowski D, Młynarczak PA, Dudziak B, Gościański M, Bartkowska A (2015) Microstructure, microhardness and corrosion resistance of Stellite-6 coatings reinforced with WC particles using laser cladding. Opt Laser Technol 68:191–201
11. Przestacki D (2014) Conventional and laser assisted machining of composite A359/20SiCp. Procedia CIRP 14:229–233
12. Rui-song J., Wang., et. al. (2016),Experimental investigation on machinability of in situ formed TiB2 particles reinforced Al MMCs. J of ManufProce 23: 249–257
13. Przestacki D, Szymanski P, Wojciechowski S (2016) Formation of surface layer in metal matrix composite A359/20SiCP during laser assisted turning. Composites Part A 91:370–379
14. Han J, Hao X, Li L, Wu Q, He N (2017) Milling of high volume fraction SiCp/Al composites using PCD tools with different structures of tool edges and grain sizes. J Adv Manuf Technol 1–8
15. Przestacki D, Chwalczuk T, Wojciechowski S (2017) The study on minimum uncut chip thickness and cutting forces during laser-assisted turning of WC/NiCr clad layers. Int J Adv Manuf Technol. doi:10.1007/s00170-017-0035-5
16. Chamanfar A, Jahazi M, Gholipour J, Wanjara P, Yue S (2015) Analysis of integrity and microstructure of linear friction welded Waspaloy. Mater Charact 104:149–161
17. Moat RJ, Pinkerton AJ, Li L, Withers PJ, Preuss M (2009) Crystallographic texture and microstructure of pulsed diode laser-deposited Waspaloy. Acta Mater 57:1220–1229
18. Mumtaz KA, Erasenthiran P, Hopkinson N (2008) High density selective laser melting of Waspaloy. J Mater Process Technol 195: 77–87

19. Razavi RS (2016) Laser beam welding of Waspaloy: characterization and corrosion behavior evaluation. Opt Laser Technol 82:113–120
20. Ding H, Shin YC (2013) Improvement of machinability of Waspaloy via laser-assisted machining. Int J Adv Manuf Technol 64:475–486
21. Davis JR (2010) Heat resistant materials. ASM International 357–369
22. Tadavani SA, Razavin RS, Vafaei R (2017) Pulsed laser-assisted machining of Inconel 718 superalloy. Opt Laser Technol 87:72–78
23. Yao-Jian L, Jia L, An L, Xiao-Tong P, Hua-Ming W (2017) Solidification path of single-crystal nickel-based superalloys with minor carbon additions under laser rapid directional solidification conditions. Scripta Mater 127:58–62
24. Yinghong L., Liucheng Z. et. al. (2013), The strengthening mechanism of a nickel-based alloy after laser shock processing at high temperatures, Sci Technol Adv Mater 14, 055010: 1–9